

1 **A Metabolic Biomarker Panel for Congenital Heart Disease Assessment**
2 **with Newborn Dried Blood Spots**

3 Scott R. Ceresnac^{1*}, Yaqi Zhang^{2,3*}, Kuo Jung Su⁴, Qiming Tang⁴, Bo Jin⁴,
4 James Schilling⁴, C. James Chou³, Zhi Han³, Brendan J. Floyd⁵, John C.
5 Whitin⁵, Karl G Sylvester³, Henry Chubb¹, Ruben Y. Luo⁶, Lu Tian⁷, Harvey J.
6 Cohen⁵, Doff B. McElhinney¹, Xuefeng B. Ling^{3*}

7

8 ¹Department of Cardiothoracic Surgery, Stanford University, Stanford, CA,
9 United States

10 ²School of Electrical Power Engineering, South China University of
11 Technology, Guangzhou, China

12 ³Department of Surgery, Stanford University, Stanford, CA, United States

13 ⁴mProbe Inc, Palo Alto, CA, United States

14 ⁵Department of Pediatrics, Stanford University, Stanford, CA, United States

15 ⁶Department of Pathology, Stanford University, Stanford, CA, United States

16 ⁷Department of Data Science, Stanford University, Stanford, CA, United States

17

18

19 *Corresponding Author:

20 ceresnak@stanford.edu, yaqizhang@gpnu.edu.cn, bxling@stanford.edu

21 **Abstract**

22 **Background:** Congenital heart disease (CHD) represents a significant
23 contributor to both morbidity and mortality in neonates and children. The
24 prompt recognition of CHD can facilitate timely and appropriate intervention,
25 reducing the probability of complications and enhancing the prognosis for
26 impacted newborns. However, unlike other rare conditions routinely identified
27 through federal and state newborn screening (NBS) programs, there's
28 currently no analogous dried blood spot (DBS) screening for CHD immediately
29 after birth.

30 **Objective:** This study was set to identify reliable metabolite biomarkers with
31 clinical relevance, with the aim to assess feasibility of screening and subtype
32 classification of CHD utilizing the DBS newborn screening method.

33 **Methods:** We assembled a cohort of DBS datasets from the California
34 Department of Public Health (CDPH) Biobank, encompassing both normal
35 controls and three pre-defined CHD categories (tetralogy of Fallot, inherited
36 arrhythmia syndrome, neonatal cardiomyopathy). A robust, DBS-oriented
37 metabolomic method, employing both global and targeted strategies based on
38 liquid chromatography with tandem mass spectrometry (LC-MS/MS), was
39 developed. To verify the reliability of this metabolic profiling, we conducted a
40 correlation analysis comparing the absolute quantitated metabolite
41 concentration in DBS against the CDPH NBS records. Additionally, for
42 hydrophilic and hydrophobic metabolites, we executed significant pathway and
43 metabolite analyses respectively. Finally, logistic and LightGBM models were
44 established to aid in CHD discrimination and classification.

45 **Results:** Our metabolomic workflow demonstrated consistent and reliable
46 quantification of metabolites in DBS samples stored at the California
47 Department of Public Health (CDPH) for up to 15 years. Through this process,
48 we discerned dysregulated metabolic pathways in CHD patients, including
49 deviations in lipid and energy metabolism, as well as oxidative stress pathways.
50 Furthermore, we identified three metabolites as potential biomarkers for CHD
51 assessment, and an additional twelve metabolites as potential markers for
52 classifying different CHD subtypes within DBS samples.

53 **Conclusions:** This study represents the first attempt to validate metabolite
54 profiling results using long-term storage DBS samples procured from the
55 high-quality conditions of the CDPH biobank. The results unveil distinct
56 metabolic discrepancies between various CHD subtypes and healthy controls.
57 Furthermore, our findings highlight the potential clinical applications of our
58 DBS-based methods for CHD screening and subtype classification.

59

60 Introduction

61 Congenital heart disease (CHD) ranks as the most prevalent form of
62 congenital anomalies^{1,2}, making it a significant contributor to morbidity and
63 mortality^{3,4}, among neonates and children. With its birth prevalence on an
64 upward trend, CHD has evolved into a major global health concern.

65 The importance of early diagnosis is paramount for the effective CHD
66 intervention and treatment. Prenatal diagnosis and early detection
67 advancements have contributed to a gradual decline in the mortality rate
68 associated with CHD in children⁵. Various screening approaches for the
69 detection of cyanotic congenital heart disease have been implemented and
70 examined, including neonatal pulse oximetry screening⁶ and universal ECG
71 screening^{7,8}. However, these methodologies exhibit less than 75% sensitivity
72 in detecting critical CHD, presenting limitations in the detection of an array of
73 congenital malformations, cardiomyopathic disorders, and inherited arrhythmia
74 syndromes. These conditions contribute significantly to neonatal mortality and
75 sudden death in children and adolescents⁹. Currently, there is no
76 comprehensive, cost-effective screening method available at birth that can
77 reliably and consistently detect the diverse range of CHD conditions that could
78 potentially harm infants and children later in life.

79 Over the past decade, the application of cardiac-specific biomarkers,
80 proteomic and metabolite analysis, mRNA, and small molecule screens has
81 seen a significant increase¹⁰⁻¹². The discovery of biomarkers associated with
82 cardiac dysfunction, myocardial cell damage, and heart-specific tissue
83 damage heralds a shift in our approach to screening, assessing, and treating

84 cardiac diseases. It has been shown that structural abnormalities, such as the
85 metabolism of acylcarnitines¹³, can create detectable metabolomic
86 disturbances. Physiological alterations linked to cyanosis in cyanotic
87 congenital heart disease, hemodynamic changes tied to volume and pressure
88 loading in non-cyanotic lesions, tissue injury due to perfusion abnormalities in
89 cardiomyopathic states, and cellular changes related to potassium, calcium,
90 and sodium exchange defects in channelopathies, could all lead to
91 distinguishable differences in the metabolomic profiles of neonates and
92 children with cardiac disease¹⁴⁻¹⁸.

93 Routine neonatal screening serves as a tool to identify diseases that could
94 potentially impact a child's long-term health or survival. Each year, millions of
95 infants in the United States undergo newborn screening (NBS), where
96 substances in dried blood spots (DBS) are measured to check for certain
97 genetic, endocrine, and metabolic disorders¹⁹. Early detection, diagnosis, and
98 intervention can avert death or disability, enabling children to reach their full
99 potential. Despite this, no DBS newborn screening exists for CHD at birth.

100 Our core hypothesis proposes that deep phenotyping of DBS metabolites at
101 birth through liquid chromatography-mass spectrometry (LC-MS) could model
102 and assess cardiac and other organ anomalies with high precision. This
103 hypothesis was previously tested with our DBS analyses assessing other
104 neonatal diseases²⁰.

105 In this study, we developed an LC-MS based metabolic screening method to
106 construct a baseline for neonate DBS metabolites and identify a DBS
107 biomarker panel as a molecular surrogate to assess congenital cardiac

108 abnormalities. Our findings attest to the robustness of our DBS-based LC-MS
109 workflow, supporting the idea that assessing DBS metabolomic biomarkers
110 may present a cost-effective and sturdy approach to evaluating the risk of CHD
111 at birth. Further understanding the functional significance of these CHD
112 biomarkers could provide fresh insights into the pathophysiology of CHD.

113 **Methods**

114 **Ethics statement**

115 This DBS NBS method development study involving human participants was
116 reviewed and approved by ethics committees at Stanford University.

117 **Study design**

118 The workflow for this study, as depicted in Fig. 1, was based on the collected
119 dried blood spot (DBS) samples. Both global **hydrophilic/hydrophobic** and
120 targeted liquid chromatography-tandem mass spectrometry (LC-MS/MS)
121 metabolomic assays were conducted, adhering to the NBS DBS processing
122 method. To verify the reliability of the metabolic profiling from samples that had
123 been stored for years, a correlation analysis was carried out comparing the
124 absolutely-quantified metabolite concentration with the California Department
125 of Public Health (CDPH) gold standard. We identified significant metabolic
126 pathways and features related to CHD and its subtypes. Finally, models for
127 CHD diagnosis and subtyping were established to validate the effectiveness of
128 the CHD-associated metabolic biomarker panel within the DBS samples.

129 **Cohorts**

130 We randomly assembled a retrospective cohort of DBS profiling datasets from
131 the CDPH Biobank. These DBS samples had been stored for up to 15 years
132 since the time of newborn testing analysis, consented to be preserved at -20°C
133 in the CDPH Biobank. In total, we included 20 clinical DBS samples, consisting
134 of 5 healthy controls (HC) and 15 cases of CHD spanning different categories.
135 The 15 CHD cases included 4 instances of Tetralogy of Fallot (TOF), 5 cases
136 of inherited arrhythmia syndromes (IAS), and 6 instances of cardiomyopathies
137 (CMP).

138 Sample preparation

139 The DBS samples were retrieved from -20°C freezers and thawed on ice. Each
140 DBS sample was cut into 3mm diameter sections, and two of these sections
141 were transferred into the same Eppendorf tube.

142 **Global hydrophilic and targeted metabolomics**

143 We followed our previously developed standard operational protocols²¹ of
144 global hydrophilic and targeted metabolomics for the workflow in this study,
145 including sample preprocessing, mass spectrometry signal acquisition, quality
146 control, data pre-processing, and metabolite biomarker structural identification.

147 For global hydrophilic metabolomics, a mixture of 250 µL extraction buffer
148 (pre-chilled to -20 °C) consisting of methanol, acetonitrile and ddH₂O (5:3:2
149 v/v) was added to each tube containing DBS punches. Samples were vortexed
150 and centrifuged at 10,000 g for 10 min at 4°C. Supernatant (180 µL) from each
151 sample was transferred into a clean Eppendorf tube. 100 µL of each sample

152 extract was transfer into an auto-sampler vial for UHPLC-MS (Ultra-High
153 Performance Liquid Chromatography) analysis.

154 For targeted metabolomics, a mixture of 200 μ L methanol / acetonitrile (1:1, v/v)
155 was added into the tube containing DBS punches. Samples were vortexed
156 vigorously and centrifuged at 10,000 g for 10 min at 4°C. The supernatant of
157 each sample was transferred into a new tube and dried under nitrogen stream.
158 10 μ L of Internal Standard Solution, 90 μ L of Extraction Buffer, and 200 μ L
159 hexane were added into the reconstituted tube for extraction. The sample was
160 vortexed vigorously for 1 min and centrifuged at 12,000 g for 5 min. 180 μ L of
161 upper layer was transferred into another 1.5-mL centrifugal tube and dried
162 under nitrogen stream again. The residue was reconstituted with 100 μ L of
163 Derivatization Buffer. The reconstituted sample was incubated at 95°C for 15
164 min. After derivatization, 100 μ L of each reconstituted sample was transferred
165 into an auto-sampler vial for the analysis of fatty acids. 80 μ L of lower layer
166 was transferred into an auto-sampler vial for the analysis of amino acids and
167 acylcarnitines.

168 **Global hydrophobic metabolomics**

169 For global hydrophobic metabolomics, a mixture of 400 μ L of chloroform /
170 methanol (1:1, v/v) and 200 μ L of water with lithium chloride were added to
171 each tube containing DBS punches. Afterwards, the sample was vortexed
172 rigorously for 30 sec and centrifuged at 12,000 g for 5 min. The bottom layer of
173 each sample was transfered into another tube. The top layer was re-extracted
174 with 400 μ L of chloroform and vortexed for 30 sec and centrifuged at 12,000 g
175 for 5 min. The bottom layer was removed and combined with extract from

176 previous trial. The combined extract was dried under nitrogen and
177 reconstituted with 100 μ L of methanol: chloroform (1:1, v/v). Thereafter, the
178 DBS extract was transferred into auto-sampler vial with micro-insert for LC/MS
179 analysis.

180 For global hydrophobic metabolomics, 5 μ L of DBS extract was injected via a
181 Vanquish UHPLC system. The mobile phase was methanol with 10 mM
182 ammonium acetate at a flow rate of 0.1 mL/min for a total run time of 3 minutes.
183 The conditions of ionization source were set at 3.4 kV for spray voltage, 15 for
184 sheath gas, 5 for aux gas, 325°C for capillary temperature, 55 for S-lens, and
185 250°C for vaporizer temperature. The MS spectra were acquired with 2 scans
186 using an AGC target of 1e6 and a resolution of 120,000 (FWHM at 200 m/z)
187 from 200 to 1200 m/z. The column oven was maintained at 25°C throughout
188 the analysis.

189 Metabolic pathway enrichment analysis with global hydrophilic and
190 hydrophobic metabolomics

191 To carry out pathway enrichment analysis on both hydrophilic and hydrophobic
192 mass spectrometric profiling results, a univariate analysis was utilized to
193 compute the fold change and p-value (using Student's t-test) for each
194 component across the three different CHD subtypes. Following the correction
195 for false discovery, components that showed significant changes (adjusted
196 p-value < 0.05) were chosen for subsequent analysis.

197 All significantly altered hydrophilic metabolites were categorized into KEGG
198 pathways²² for further examination, while significantly changed hydrophobic

199 metabolites were grouped into the Lipid Map database²³. Enriched pathways
200 of significance were identified with a Fisher's exact test p-value of < 0.05.

201 **Statistic learning for multi-class classification**

202 Orthogonal partial least squares discriminant analysis (OPLS-DA) was
203 performed using global hydrophilic and hydrophobic metabolic profiling results.
204 Unsupervised clustering results were used to visualize the two-dimensional
205 clustering patterns of HC, TOF, IAS and CMP DBS samples. With OPLS-DA
206 results, the performance of the discrimination between two of these DBS
207 sample categories was assessed using a receiver operating characteristic
208 curve (ROC) and the area under the curve (AUC).

209 To distinguish between CHD patients and healthy controls, a logistic model²⁴
210 was constructed based on targeted metabolomic profiling results. For CHD
211 subtyping, the importance of identified targeted metabolites was determined
212 using a gradient boosting machine provided by the LightGBM library²⁵.
213 Analysis was implemented with default parameters, and the metric used for
214 early stopping was set to the error rate for multi-class classification²⁶.
215 Metabolites were then ranked based on their normalized importance scores.
216 Metabolites with cumulative importance greater than 80% were selected as
217 biomarkers.

218 The significantly relevant biomarker metabolites associated with CHD
219 diagnosis and subtyping were then proposed and discussed.

220 **Results**

221 Demographics and Clinical Characteristics

222 **Table 1** summarizes the cohort demographics and clinical characteristics. This
223 includes a cohort of 20 neonates, comprising of 5 controls and 15 CHD
224 patients. Of these 20 neonates, 11 were boys (55%) and 9 were girls (45%).
225 The 15 CHD patients comprised 4 diagnosed with CHD-Tetralogy of Fallot
226 (TOF), 5 with CHD-inherited arrhythmia syndromes (IAS (2 Brugada, 3 Long
227 QT syndrome)), and 6 with CHD-cardiomyopathies (CMP (3 dilated, 3
228 hypertrophic cardiomyopathy)). No statistically significant differences were
229 observed in the distribution of gender and race across all groups.

230 The DBS samples had been stored in the CDPH biobank at -20 °C for up to 15
231 years, as shown in Fig. 2. We reanalyzed the concentrations of 28 metabolites,
232 which are common to the CDPH DBS NBS records (Table 1) and include
233 amino acids, free carnitines, and acylcarnitines. Fig. 3 shows that 24 out of the
234 28 metabolites exhibit a strong correlation, affirming both the robustness of our
235 metabolomic profiling workflow and the reliability of these DBS samples even
236 after many years of storage.

237 Exploration of the unique metabolic patterns among different CHD subtypes

238 Two distinct high-throughput global mass spectrometric workflows were
239 conducted, focusing on hydrophilic and hydrophobic metabolites separately.
240 After data preprocessing, a total of 1829 compounds were identified in the
241 global hydrophilic metabolomic profiling, and 1383 compounds were identified
242 in the global hydrophobic metabolomics.

243 Multivariate analysis, specifically sparse partial least squares discriminant
244 analysis (OPLS-DA), was then performed on the global hydrophilic and
245 hydrophobic metabolomics to investigate different CHD subtypes, including
246 TOF, IAS, and CMP. The results, presented in **Fig. 4** and **Table 2**, revealed
247 distinct clustering patterns for samples from various CHD subtypes in both the
248 global hydrophilic and hydrophobic metabolic profiling.

249 Interestingly (**Fig. 4** and **Table 2**), CHD-IAS could not be reliably distinguished
250 from other groups (ROC AUC, 0.607; P value, 0.458) based on the global
251 hydrophilic metabolomics, while CHD-CMP also showed poor distinction from
252 other groups (ROC AUC, 0.533; P value, 0.827) based on the global
253 hydrophobic metabolomics. These findings suggest that each CHD subtype
254 may indeed exhibit unique metabolic differences compared to both the healthy
255 control and other CHD subtype groups.

256 **Pathway analysis with global hydrophilic and hydrophobic** 257 **metabolomics**

258 To identify specific metabolic differences in CHD subtypes, pathway
259 enrichment analysis was performed on the significant changes observed in
260 global metabolism (adjusted P value < 0.05) (Fig. 5). For hydrophilic
261 metabolites, the KEGG pathway database was utilized, while the Lipids Map
262 database was used for hydrophobic metabolites. The results depicted in Fig. 5
263 show that the Arachidonic acid metabolism and Monoradylglycerols pathways
264 are consistently and significantly enriched in all three CHD subtypes.
265 Additionally, the Linoleic acid metabolism, serotonergic synapse, and
266 sphingoid bases pathways are significantly enriched solely in the IAS and TOF

267 subtypes of CHD. Moreover, Quinones and hydroquinones were found to be
268 significantly enriched only in CHD-CMP, while Arginine and ornithine
269 metabolism showed significant enrichment exclusively in CHD-IAS. These
270 findings suggest the presence of diverse metabolic pathway changes among
271 the different CHD subtypes, emphasizing the importance of considering both
272 hydrophilic and hydrophobic metabolites when constructing a CHD diagnosis
273 panel. Such a comprehensive approach will enable a more accurate and
274 informative characterization of the metabolic profiles associated with different
275 CHD subtypes.

276 Identification of a metabolic signature for CHD

277 Using our targeted metabolomics methods, we conducted quantitative
278 measurements of 836 targeted metabolites and lipids in DBS samples
279 collected from both CHD patients and healthy controls. Upon comparing CHD
280 patients with healthy controls, we identified 3 biomarker metabolites ($p < 0.05$)
281 through univariate analysis, namely PC(d16:1-22:3), C14:1-Carnitine, and
282 C12-Carnitine (**Fig. 6A** and **Fig. 6B**).

283 To further explore the diagnostic potential of these biomarkers, we constructed
284 a logistic model based on their concentrations. This logistic model exhibited
285 high accuracy in distinguishing between CHD patients and healthy controls,
286 achieving an area under the curve (AUC) of 0.982 (95% CI: 0.92-1.00) (**Fig.**
287 **6C**). The sensitivity and specificity of this logistic model were 92.8% and
288 75.0%, respectively.

289 Regarding the metabolic signature for CHD subtyping, we employed the
290 LightGBM model to calculate the importance of each metabolite in the
291 multiclass classification of the three types of CHD. This analysis revealed 12
292 crucial metabolites required to achieve 80% cumulative importance (**Fig. 6D**).
293 These significant metabolites include Alanine, C10-Carnitine,
294 TG(16:0-16:0-20:2), TG(16:1-18:2-18:3), PE(a20:0-20:2), C10:1-Carnitine,
295 Octacosanoic acid(28:0), C14:1OH-Carnitine, C8:1-Carnitine, Asparagine,
296 C0-Carnitine, and d18:0 CE.

297 Following that, OPLS-DA analysis was carried out using the aforementioned
298 12 metabolites (**Fig. 6E**). The results, as shown in **Fig. 7**, revealed an AUC of
299 0.963 (P value = 0.03) for distinguishing CMP vs Other, an AUC of 0.98 (P
300 value = 0.03) for distinguishing IAS vs Other, and an AUC of 0.84 (P value =
301 0.05) for distinguishing TOF vs Other. These findings indicate promising
302 discriminatory capabilities of the selected metabolites in identifying different
303 CHD subtypes when compared to the other groups.

304 **Discussion**

305 **Summary of main findings**

306 To explore the identification of CHD metabolic biomarkers using dried blood
307 DBS samples, we began by verifying the reliability of the metabolic profiling
308 from these samples, even after years of storage. This was achieved through
309 correlation analysis of the absolute quantitated metabolite concentrations from
310 this study and the CDPH database records. Subsequently, utilizing global and

311 targeted LC-MS/MS metabolomic profiling methods, we further analyzed the
312 significant metabolic pathways associated with CHD and its subtypes.
313 In the process, we established models for CHD diagnosis and subtyping to
314 validate the effectiveness of the CHD-associated metabolic patterns. Our
315 findings revealed distinct metabolic differences in significant pathways and
316 unique metabolic patterns related to both CHD and its subtypes. Furthermore,
317 using targeted metabolomics, we identified 3 biomarker metabolites for CHD
318 diagnosis and 12 biomarker metabolites for CHD subtyping. These results
319 support the hypothesis that serial LC-MS profiling of DBS metabolites from
320 newborns may hold potential in accurately assessing CHD and offer a
321 non-invasive and cost-effective method for CHD detection.

322 Overall, this study sheds light on the potential of utilizing metabolic profiling
323 from DBS samples as a precise and efficient means of CHD diagnosis, paving
324 the way for improved early detection and management of this condition.

325 **The stability of amino acid and acyl carnitines in DBS**

326 In this study, we utilized CHD DBS samples obtained from the CDPH Biobank,
327 an invaluable resource for research due to its extensive collection of biological
328 specimens suitable for various types of investigations, including
329 epidemiological, genetic, and biomarker research. However, concerns
330 regarding the stability and quality of samples stored in biobanks over extended
331 periods have been raised, limiting retrospective analyses using stored DBS.

332 To address this concern and ensure the accuracy and reliability of
333 metabolomic studies, we focused on assessing the stability of acylcarnitines
334 and amino acids in DBS stored in freezers after newborn screening. Our
335 research aimed to shed light on the long-term stability of these metabolites in
336 stored specimens.

337 The encouraging findings of our study revealed excellent stability for both
338 amino acids and acyl carnitines, even after up to 15 years of storage. This
339 discovery provides reassurance that dried blood specimens stored in the
340 CDPH biobank freezers can be reliably used for metabolomic studies, even
341 following prolonged storage. This insight enhances the confidence in utilizing
342 the biobank's stored samples for future investigations, contributing to the
343 advancement of CHD and other related research areas.

344 **CHD biomarker biological implications**

345 Informative alterations in plasma metabolite concentrations related to specific
346 metabolic pathways have been found to be associated with the CHD
347 pathogenesis and pathophysiology²⁷. A notable example is the significant
348 involvement of fatty acid metabolism in hypertrophied newborn hearts, where it
349 plays a crucial role in energy generation²⁸. In our investigation, we discovered
350 a significant association between the arachidonic acid (AA) metabolism
351 pathway and the pathophysiology of various CHD subtypes, including TOF,
352 IAS, and CMP (**Fig. 5A**). The AA metabolism pathway is intricate, involving the
353 metabolism of arachidonic acid, an omega-6 fatty acid, by enzymes like
354 cyclooxygenases (COX), lipoxygenases (LOX), and cytochrome P450 (CYP)
355 enzymes. This pathway gives rise to diverse bioactive lipid mediators, such as

356 prostaglandins, thromboxanes, leukotrienes, and epoxyeicosatrienoic acids
357 (EETs), which play essential roles in various physiological and pathological
358 processes²⁹.

359 Previous studies have demonstrated that dysregulation of the AA metabolism
360 pathway is linked to the development and progression of CHD. For instance, in
361 TOF, a common CHD type, there is evidence of increased oxidative stress and
362 inflammation^{30,31}, leading to potential dysregulation of the AA metabolism
363 pathway. Such dysregulation could result in the overproduction of
364 vasoconstrictive and pro-inflammatory mediators, such as thromboxane A2
365 and leukotriene B4, contributing to pulmonary hypertension and exacerbating
366 right ventricular dysfunction^{32,33}. Similarly, in inherited arrhythmia syndromes
367 like long QT syndrome and Brugada syndrome, genetic mutations in ion
368 channel genes can alter AA metabolism and lead to the production of EETs.
369 These EETs can modulate ion channel activity, affecting cardiac repolarization
370 and leading to arrhythmias and sudden cardiac death³⁴⁻³⁶. In cardiomyopathies
371 such as hypertrophic cardiomyopathy and dilated cardiomyopathy, elevated
372 inflammation and fibrosis have been observed, potentially contributing to the
373 dysregulation of the AA metabolism pathway^{37,38}. Consequently, the
374 overproduction of pro-inflammatory and pro-fibrotic mediators, such as
375 prostaglandin E2 and leukotriene B4, may play a role in cardiac remodeling
376 and dysfunction. Overall, our findings highlight the relevance of the AA
377 metabolism pathway in CHD pathogenesis and shed light on its potential as a
378 target for further research and therapeutic interventions.

379 Pathway enrichment analysis conducted on the global metabolic profiling
380 revealed a particularly significant change in the linoleic acid (LA) metabolic
381 pathway in TOF and IAS, while no substantial change was observed in CMP
382 (**Fig. 5A**). It's worth noting that the LA pathway and AA pathway are closely
383 interrelated. The metabolism of linoleic acid involves a series of enzymatic
384 reactions that ultimately lead to the production of arachidonic acid (AA) and its
385 derivatives, including prostaglandins and leukotrienes, which play pivotal roles
386 in inflammation, cardiovascular function, and other physiological processes.
387 Recent studies have indicated that the linoleic acid pathway may play a role in
388 the development of coronary heart disease [39]. Specifically, research
389 suggests that mutations in the gene responsible for coding delta-6 desaturase
390 (D6D), the enzyme responsible for converting linoleic acid to arachidonic acid,
391 could be associated with an increased risk of coronary heart disease³⁹.
392 Furthermore, LA metabolism may also interact with other molecular pathways
393 involved in cardiac development, such as the Wnt signaling pathway, which
394 has been implicated in CHD pathogenesis⁴⁰⁻⁴². Although the exact
395 mechanisms by which dysregulation of the LA metabolism pathway contributes
396 to CHD are not yet fully understood, the linoleic acid metabolism pathway has
397 emerged as a potential contributor to the pathogenesis of congenital heart
398 disease. These findings highlight the importance of further research into this
399 metabolic pathway and its potential implications in CHD development and
400 progression.

401 Monoradylglycerols (MG) are a type of lipid molecule characterized by a
402 glycerol backbone with a single fatty acid molecule attached to it. These lipids
403 are commonly found in various foods, particularly in processed foods that

404 contain added fats and oils. Currently, there is no direct evidence to suggest
405 that MG are directly linked to the development of CHD. However, studies have
406 demonstrated that a diet high in saturated fats, often found in processed foods
407 containing MG, may indeed increase the risk of developing CHD. High-fat diets
408 in expectant mothers have been shown to enhance the expression of placental
409 mRNA associated with the arachidonic acid (AA) metabolism pathway⁴³. This
410 can lead to elevated fetal arachidonic acid levels due to maternal arachidonic
411 acid transfer, resulting in an upregulation of fetal VEGF expression⁴⁴.
412 Consequently, an overexpression of VEGF in the myocardium may impede the
413 process of epithelial-mesenchymal transformation, which is crucial for
414 endocardial cushion formation. Such impairment of endocardial cushion
415 formation can trigger defects in septation and outflow tract development⁴⁵. In
416 this context, Smedts et al. reported that a high maternal intake of saturated fat
417 is associated with a higher likelihood of developing outflow tract defects⁴⁶.
418 Furthermore, these researchers found that infants born to mothers with
419 abnormal lipid profiles have twice the risk of CHD⁴⁷. While MG themselves
420 may not be directly linked to CHD, their presence in processed foods that are
421 high in saturated fats may contribute to an increased risk of developing CHD
422 over time. In conclusion, while MG are not directly implicated in CHD
423 development, their association with processed foods high in saturated fats
424 underscores the importance of dietary considerations in reducing the risk of
425 CHD. Adopting a balanced and healthy diet may help mitigate potential risks
426 associated with the consumption of saturated fats and processed foods.

427 The QHJ pathway is a vital metabolic pathway responsible for maintaining
428 cellular homeostasis and safeguarding cells against oxidative stress. Its

429 primary function involves regulating the redox balance in cells by converting
430 quinones to hydroquinones, which helps control oxidative stress. Oxidative
431 stress arises when there is an imbalance between reactive oxygen species
432 (ROS) production and the cellular antioxidant defense system. Excessive ROS
433 production can lead to oxidative damage of cellular components, such as DNA,
434 proteins, and lipids, ultimately resulting in cellular dysfunction and cell death.
435 This oxidative stress condition has been implicated in the pathogenesis of
436 various diseases, including CHD. Prior studies have highlighted the
437 involvement of oxidative stress in the development of heart malformations,
438 impaired cardiac function, and other complications associated with CHD⁴⁸.
439 Both cyanotic and acyanotic congenital heart diseases have been shown to
440 induce a pro-oxidant state in the human body, leading to increased levels of
441 total antioxidants, oxidants, and the oxidative stress index in affected
442 children^{49,50}. In our study, we observed that the QHQ pathway showed
443 significant differences only in CMP patients (**Fig. 5B**). However, further
444 research is warranted to fully comprehend the underlying mechanisms by
445 which oxidative stress contributes to CHD development. Additionally,
446 identifying potential markers for the early diagnosis of this condition could be
447 crucial in advancing CHD management and treatment strategies. In summary,
448 the QHQ pathway's involvement in cellular redox regulation and oxidative
449 stress highlights its potential significance in CHD pathogenesis. Understanding
450 its role could provide valuable insights into the development and progression
451 of CHD and pave the way for novel therapeutic interventions and diagnostic
452 approaches.

453 Furthermore, our study involved targeted metabolomics to profile amino acids,
454 acylcarnitines, and lipids, given their central role in the pathogenesis of heart
455 disease. Carnitine and acylcarnitines play critical roles in energy metabolism,
456 especially in the transport of long-chain fatty acids into the mitochondria for
457 energy production. Infants with CHD are particularly susceptible to energy
458 imbalances, and although most of them have normal weight at birth, they often
459 experience nutritional and growth problems in early infancy⁵¹. This has spurred
460 growing interest in investigating the potential of carnitine and acylcarnitine for
461 the diagnosis and management of CHD. Several studies have reported
462 decreased levels of carnitine and acylcarnitines in patients with CHDs,
463 particularly those with ventricular overload or pulmonary hypertension^{52,53}.
464 These decreases may indicate impaired cardiac metabolism and energy
465 production, which can contribute to the development of cardiomyopathy and
466 other complications. Beyond carnitine and acylcarnitines, Bahado-Singh et al.
467 conducted a study examining phosphatidylcholine (PC) levels in CHD patients.
468 PC is a major component of cell membranes and is vital for cell structure and
469 function. In the context of CHD, disturbances in tissue remodeling may impact
470 the rate of cell membrane synthesis and destruction, leading to abnormal
471 choline and PC metabolism. Their study revealed significant abnormalities in
472 phosphatidylcholine (PC) and lipid levels in the serum of pregnant women
473 carrying CHD fetuses during the first trimester. Additionally, disturbances in
474 carnitine levels and lipid synthesis were identified, potentially linked to
475 single-carbon metabolism through choline⁵⁴. Consistent with these studies, our
476 research unveiled statistically significant alterations in acylcarnitine and PC
477 levels in DBS samples of CHD patients compared to those of healthy children.

478 Specifically, we identified C12-carnitine, C14:1 carnitine, and PC(d16:1-22:3)
479 as potential diagnostic markers for CHD. These findings provide valuable
480 insights into the metabolic changes associated with CHD and may offer
481 promising avenues for improved diagnosis and management of this condition.

482 Limitations

483 While our study shows promising potential for metabolomics in CHD newborn
484 screening, it is essential to acknowledge several limitations that may influence
485 the interpretation of our findings. One of the primary limitations is the small
486 sample size used in our study, which may limit the representativeness of our
487 results to a broader population. To enhance the reliability and generalizability
488 of our findings, future research should strive to include larger cohorts, allowing
489 for more robust statistical analysis and validation of the identified biomarkers.
490 Furthermore, it is worth noting that our study was conducted at a specific
491 location, California, USA, which could introduce potential biases related to
492 sample collection, processing, and data analysis. To overcome this limitation
493 and increase the external validity of our findings, conducting multicenter
494 studies in different regions with diverse populations would be highly beneficial.
495 Another important limitation of our study is the lack of consideration for
496 potential confounding factors that may influence the identified biomarkers.
497 Factors such as prenatal exposures, maternal health, and perinatal variables
498 could have an impact on the metabolic signature of CHD. Future research
499 should take these confounders into account to gain a more comprehensive
500 understanding of their influence on metabolomic profiles in CHD. In conclusion,
501 while our study provides valuable insights into the potential of metabolomics in

502 CHD screening, it is crucial to recognize and address these limitations in future
503 investigations. By doing so, we can further enhance the reliability and
504 applicability of metabolomics in early CHD detection and potentially improve
505 patient outcomes.

506 **Conclusion**

507 Newborn screening using tandem mass spectrometry has been widely
508 adopted as a public health strategy in developed countries to detect inborn
509 errors of metabolism. However, its sensitivity for detecting critical congenital
510 heart disease (CHD) remains relatively low, necessitating the urgent
511 exploration of CHD-related biomarkers. In our study, we have made significant
512 progress in this area. Our research has demonstrated the excellent stability of
513 amino acids and acyl carnitines in dried blood spots (DBS) even after
514 extended storage of up to 15 years. Leveraging this stability, we identified
515 dysregulated metabolic pathways in CHD patients, including alterations in lipid
516 metabolism, energy metabolism, and oxidative stress pathways. Furthermore,
517 through targeted metabolomics, we successfully uncovered potential
518 diagnostic biomarkers, such as acylcarnitines and phosphatidylcholine (PC).
519 These identified biomarker metabolites associated with CHD diagnosis and
520 subtyping hold promising potential as a metabolic signature for CHD newborn
521 screening. This exciting finding opens the door to potential clinical applications
522 of metabolomics in facilitating early CHD detection and assessment, utilizing
523 dry blood spot samples. Moreover, by further investigating the biomarker
524 metabolites and their underlying enriched pathways, we may gain deeper
525 insights into the mechanisms underlying CHD pathophysiology. This can lead

526 to a better understanding of CHD development, which has implications for
527 future research, treatments, and improved patient outcomes. In conclusion,
528 our study highlights the significant progress made in the application of
529 metabolomics for CHD newborn screening and the identification of potential
530 biomarkers. By unraveling the metabolic changes associated with CHD, we
531 can move closer to developing effective screening methods and enhancing our
532 understanding of CHD's pathogenesis.

533 **Tables**

534 **Table 1.** The demographics of CDPH DBS Samples.

Characters	Control	CHD			P-value
		TOF	IAS	CMP	
Total	5	4	5	6	
Diagnosis					< 0.001
Normal	5 (100)	0 (0)	0 (0)	0 (0)	
Tetralogy of Fallot	0 (0)	4 (100)	0 (0)	0 (0)	
Brugada syndrome	0 (0)	0 (0)	2 (40)	0 (0)	
Long QT syndrome	0 (0)	0 (0)	3 (60)	0 (0)	
Dilated cardiomyopathy	0 (0)	0 (0)	0 (0)	3 (50)	
Hypertrophic cardiomyopathy	0 (0)	0 (0)	0 (0)	3 (50)	

Age					
mean (SD)	0 (0)	0 (0)	0 (0)	0 (0)	
Gender					
					0.929
Female	2 (40)	2 (50)	3 (60)	2 (33.3)	
Male	3 (60)	2 (50)	2 (40)	4 (66.7)	
Race					
					0.168
Asian	0 (0)	1 (25)	0 (0)	1 (16.7)	
Black	1 (20)	0 (0)	0 (0)	0 (0)	
Hispanic	0 (0)	1 (25)	4 (80)	3 (50)	
White	4 (80)	2 (50)	1 (20)	2 (33.3)	
CDPH DBS NBS records					
Thyroid stimulating hormone, mean (SD)	6.7 (4.7)	5.6 (5.4)	5.5 (3.9)	4.4 (1.7)	0.817
C8-Carnitine, mean (SD)	0.1 (0)	0 (0)	0.1 (0)	0.1 (0)	0.011
Galactose-1-phosphate uridyl transferase, median (IQR)	247.2 (217,267.5)	219.1 (170.6,274.6)	269.5 (260.4,271)	308.5 (304.3,314.1)	0.166
Valine, mean (SD)	105.9 (19.3)	102.7 (60.9)	114.3 (40.7)	90 (20.9)	0.74
C18:1-Carnitine, mean (SD)	1.2 (0.3)	0.9 (0.5)	1 (0.3)	1.2 (0.3)	0.513
C160H-Carnitine	0 (0)	0 (0)	0 (0)	0 (0)	0.164

/C16-Carnitine Ratio, mean (SD)					
C16:1-Carnitine, mean (SD)	0.3 (0)	0.1 (0.1)	0.2 (0.1)	0.3 (0.1)	0.02
17-Hydroxyprogesterone (17-OHP), mean (SD)	13.3 (8.9)	18.3 (8.8)	22.3 (18.6)	10.9 (3.4)	0.378
C3-Carnitine / C2-Carnitine Ratio, mean (SD)	0.1 (0)	0.1 (0)	0.1 (0)	0.1 (0)	0.291
C14-Carnitine, mean (SD)	0.3 (0)	0.2 (0.1)	0.2 (0)	0.2 (0.1)	0.005
Methionine, mean (SD)	28 (6.1)	25.5 (12.4)	20.2 (4.7)	26 (5.5)	0.397
Alanine, mean (SD)	230 (96.8)	369.8 (180.5)	307.2 (74)	307.3 (109)	0.379
Immunoreactive trypsinogen, mean (SD)	17.7 (7.7)	15.9 (2.5)	30.8 (16.1)	18.6 (8.3)	0.131
Ornithine/Citrulline Ratio, median (IQR)	5.7 (4.7,7.5)	6.5 (5.5,8.8)	4.8 (4.8,8.4)	4.6 (4.3,4.9)	0.385
Arginine/Ornithine Ratio, mean (SD)	0.1 (0)	0.1 (0.1)	0.1 (0.1)	0.1 (0.1)	0.919
Leucine/Isoleucine, median (IQR)	99.1 (93.4,113.2)	86.7 (61.2,133.5)	95.4 (62.8,106.5)	88.9 (85.2,100.7)	0.838
C12-Carnitine, mean (SD)	0.2 (0.1)	0 (0)	0.1 (0.1)	0.1 (0)	0.016
C18:2-Carnitine, median	0.1	0.3	0.1	0.2	0.278

(IQR)	(0.1,0.2)	(0.2,0.6)	(0.1,0.3)	(0.1,0.2)	
Glycine, mean (SD)	525.6 (89.3)	448 (213.7)	471.8 (105.1)	553.5 (68.6)	0.521
C6-Carnitine, mean (SD)	0.1 (0)	0 (0)	0 (0)	0.1 (0)	0.097
C5OH-Carnitine, median (IQR)	0.2 (0.1,0.2)	0.2 (0.2,0.2)	0.2 (0.2,0.3)	0.2 (0.2,0.2)	0.579
Succinylacetone, mean (SD)	0.5 (0.3)	0.2 (0.1)	0.6 (0.4)	0.4 (0.3)	0.33
C12:1-Carnitine, mean (SD)	0.1 (0.1)	0 (0)	0.1 (0.1)	0.1 (0)	0.018
Arginine	8.6 (2.6)	8.8 (7.9)	9.2 (3.1)	7.5 (6.6)	0.96
C18:1OH-Carnitine, mean (SD)	0 (0)	0 (0)	0 (0)	0 (0)	0.184
C3DC-Carnitine /C10-Carnitine Ratio, mean (SD)	1.3 (0.4)	2.7 (0.9)	1.7 (0.6)	2.1 (1.2)	0.157
FC, mean (SD)	19.6 (5.9)	28 (11.2)	25.3 (12.5)	19 (4.6)	0.352
Leucine/Alanine Ratio, mean (SD)	0.5 (0.2)	0.3 (0.1)	0.3 (0.2)	0.3 (0.1)	0.135
Citrulline/Arginine Ratio, mean (SD)	2.1 (0.9)	2.8 (2.2)	1.7 (1)	4.1 (3.4)	0.331
C14:2-Carnitine, mean (SD)	0 (0)	0 (0)	0 (0)	0 (0)	0.1
C4-Carnitine, median (IQR)	0.3 (0.2,0.3)	0.2 (0.1,0.3)	0.2 (0.2,0.3)	0.2 (0.2,0.2)	0.691

C8:1-Carnitine, mean (SD)	0.1 (0)	0.1 (0)	0.1 (0)	0.1 (0)	0.216
Phenylalanine/Tyrosine	0.6		0.7	0.6	
Ratio, median (IQR)	(0.6,0.7)	0.9 (0.9,1)	(0.7,0.8)	(0.6,0.7)	0.036
C2-Carnitine, mean (SD)	23.7 (9.8)	26.6 (11.4)	20 (4.5)	23.6 (7.2)	0.701
Biotinidase, mean (SD)	43.4 (10.3)	41.7 (5.6)	51.4 (13.8)	42.7 (7.5)	0.417
C5DC-Carnitine, mean (SD)	0.2 (0.1)	0.1 (0)	0.2 (0.1)	0.2 (0.1)	0.104
C18OH-Carnitine, median (IQR)	0 (0,0)	0 (0,0)	0 (0,0)	0 (0,0)	0.086
C3-Carnitine, mean (SD)	1.6 (0.4)	2.1 (0.9)	1.6 (0.5)	2.2 (0.6)	0.318
C18-Carnitine, mean (SD)	0.8 (0.2)	0.8 (0.2)	0.7 (0.1)	0.8 (0.2)	0.454
C14:1-Carnitine /					
C12:1-Carnitine Ratio, mean (SD)	1.3 (0.1)	1.7 (0.9)	1.2 (0.4)	1.6 (0.4)	0.51
C10-Carnitine, mean (SD)	0.1 (0)	0 (0)	0.1 (0)	0.1 (0)	0.005
C5:1-Carnitine, median (IQR)	0 (0,0)	0 (0,0)	0 (0,0)	0 (0,0)	0.51
5-Oxoproline, mean (SD)	21.8 (5)	32 (7.4)	26.8 (6.6)	25.2 (8.2)	0.221
C10:1-Carnitine, mean (SD)	0.1 (0)	0 (0)	0.1 (0)	0 (0)	0.238
C5-Carnitine, mean (SD)	0.1 (0)	0.1 (0.1)	0.1 (0)	0.1 (0)	0.978
Phenylalanine, mean (SD)	63.9 (8.2)	69.8 (33.3)	55.4 (19.7)	66.6 (15.8)	0.719
Proline, mean (SD)	203.4 (38.2)	159.8 (73.4)	180.8 (43.6)	179.2 (33.7)	0.593

C16OH-Carnitine, mean (SD)	0 (0)	0 (0)	0 (0)	0 (0)	0.032
	103.6			102.7	
Tyrosine, mean (SD)	(17.7)	72.6 (35.5)	68.7 (30.1)	(32.7)	0.15
	98.6	103.8			
Ornithine, mean (SD)	(44.5)	(92.5)	102 (53.1)	79.8 (28)	0.882
FC / (C16-Carnitine +					
C18:1-Carnitine) Ratio,	4.3 (3.9,5)	8.1 (7.3,9)	6.7 (5,7.1)	4.5 (3.7,5)	0.037
median (IQR)					
C16-Carnitine, mean (SD)	3.4 (1)	2.5 (0.9)	2.3 (0.3)	3.1 (0.8)	0.166
C14OH-Carnitine, mean (SD)	0 (0)	0 (0)	0 (0)	0 (0)	0.012
C3DC-Carnitine, mean (SD)	0.1 (0)	0.1 (0)	0.1 (0)	0.1 (0)	0.02
C14:1-Carnitine, mean (SD)	0.2 (0.1)	0 (0)	0.1 (0)	0.1 (0)	0.004
C5-Carnitine /C3-Carnitine					
Ratio, mean (SD)	0.1 (0)	0.1 (0)	0.1 (0)	0.1 (0)	0.279
C8-Carnitine /C10-Carnitine					
Ratio, mean (SD)	0.7 (0.1)	1 (0.5)	1 (0.3)	0.8 (0.1)	0.472
Citrulline, mean (SD)	16.6 (3.6)	11.8 (3.9)	14 (6)	17 (3.2)	0.242
Valine / Phenylalanine Ratio,					
mean (SD)	1.7 (0.3)	1.5 (0.4)	1.9 (0.4)	1.4 (0.3)	0.147

535 Values are mean ± SD or numbers (percentages). SD: Standard deviation; IQR:

536 Interquartile Range. CHD: Congenital heart disease. TOF: Tetralogy of Fallot. IAS:

537 Inherited arrhythmias syndromes. CMP: Cardiomyopathies.

538

539 **Table 2.** Discernibility ability to CHD subtypes by global hydrophilic and
540 hydrophobic metabolomics with orthogonal partial least squares discriminant
541 analysis (OPLS-DA) .

	Hydrophilic		Hydrophobic	
	AUC	P-value	AUC	P-value
HC vs Other(s)	1.00	0.001	1.00	0.001
CMP vs Other(s)	0.881	0.008	0.607	0.458
IAS vs Other(s)	0.533	0.827	0.987	0.001
TOF vs Other(s)	0.969	0.005	0.906	0.014

542 HC: Health Control. TOF: Tetralogy of Fallot. IAS: Inherited arrhythmias syndromes. CMP:
543 Cardiomyopathies.

544 **Figures**

545 **Figure 1.** Study workflow diagram to apply metabolomic analytics to the
546 neonate DBS samples and to discover CHD biomarkers. Abbreviations: CHD-
547 Congenital heart disease, TOF- Tetralogy of Fallot, IAS- Inherited arrhythmias
548 syndromes, CMP- Cardiomyopathies.

549 **Figure 2.** Statistical distribution of DBS Samples storage times in California
550 Department of Public Health (CDPH) Lab.

551 **Figure 3.** Impact of the time storage of metabolites. A) scatter plots showing
552 the positive correlations of metabolic profiling between this study (X-axis) and
553 the CDPH DBS records (Y-axis). B) Statistical distribution of the correlation
554 coefficient.

555 **Figure 4.** Orthogonal partial least squares discriminant analysis (OPLS-DA)
556 using the global hydrophilic and hydrophobic metabolic profiling results of
557 health control (HC), CHD-Tetralogy of Fallot (TOF), CHD-inherited arrhythmia
558 syndromes (IAS) and CHD-cardiomyopathies (CMP). A) clustering results of
559 hydrophilic metabolic profiling B) clustering results of hydrophobic metabolic
560 profiling.

561 **Figure 5.** Significant Metabolic pathways altered in different CHD subtypes.
562 Pathway enrichment analysis on the A) global hydrophilic and B) hydrophobic
563 metabolic profiling. All significant changed components (P value <0.05,
564 Student's t-test) in CHD-Tetralogy of Fallot (TOF), CHD-inherited arrhythmia
565 syndromes (IAS) and CHD-cardiomyopathies (CMP) are mapping to KEGG
566 metabolic pathways and Lipid Map database, respectively. *: P value <0.05, **:
567 P value <0.01, ***: P value <0.001.

568 **Figure 6.** The application of targeted metabolomics to discover CHD diagnosis
569 and subtyping biomarker metabolites using DBS samples. A) Volcano plots for
570 screening significant changed metabolites associated with CHD, the
571 metabolites with P value < 0.05 and fold change >1.5 are marked as red dots
572 and the metabolites with P value < 0.05 and fold change < 0.67 are marked as
573 blue dots. B) violin plots for three biomarker metabolites for CHD diagnosis. *:

574 Student's P value <0.05, **: P value <0.01, ***: P value <0.001. C) the
575 smoothed receiver operating characteristic curve (AUC ROC) of logistic model
576 based on three biomarkers. 95% confidence intervals are shown in grey lines.
577 D) the importance score of the 12 metabolites associated with CHD subtyping
578 which have an 80% cumulative importance in total. E) PLS-DA cluster results
579 using 12 metabolites for CHD subtyping.

580 **Figure 7.** CHD Subtyping modeling with targeted metabolomic profiling
581 analysis of newborn DBS samples. A) Confusion matrix. B) AUC curves to
582 demonstrate the performance to diagnose CHD subtypes.

583 **Acknowledgements**

584 The biospecimens and/or data (Request ID: 1893) used in this study were
585 obtained from the California Biobank Program (CBP) in accordance with
586 Section 6555(a), 17 CCR. The California Department of Public Health is not
587 responsible for the results or conclusions drawn by the authors of this
588 publication.

589 **Author contributions**

590 Experimental design: S.R. Ceresnac, X.B.Ling

591 Mass spectrometric assay development: X.B.Ling, Y. Zhang, K.J. Su, J.

592 Schilling, R.Y. Luo

593 Sample procurement and data entry: S.R. Ceresnac, X.B.Ling, Y. Zhang

594 Data analysis: Q. Tang, B. Jin, C.J. Chou, Z. Han, L. Tian,

595 Clinical Interpretation: S.R. Ceresnac, B.J. Floyd, K.G. Sylvester, H. Chubb,
596 H.J. Cohen, Doff. McElhinney
597 Manuscript preparation: S.R. Ceresnac, X.B.Ling, Y. Zhang, J.C. Whitin, K.G.
598 Sylvester, H. Chubb, , H.J. Cohen, D.B. McElhinney

599 **Competing interests**

600 K.J. Su, Q. Tang, J. Schilling, B. Jin are staff members of mProbe Inc. The rest
601 of the authors declare no conflict of interest. The funders had no role in the
602 design of the study; in the collection, analyses, or interpretation of data; in the
603 writing of the manuscript; or in the decision to publish the results.

604 **References**

- 605 1. Hoffman JI, Kaplan S. The incidence of congenital heart disease. *J Am Coll*
606 *Cardiol.* 2002;39:1890-1900. doi: 10.1016/s0735-1097(02)01886-7
- 607 2. van der Linde D, Konings EE, Slager MA, Witsenburg M, Helbing WA,
608 Takkenberg JJ, Roos-Hesselink JW. Birth prevalence of congenital heart disease
609 worldwide: a systematic review and meta-analysis. *J Am Coll Cardiol.*
610 2011;58:2241-2247. doi: 10.1016/j.jacc.2011.08.025
- 611 3. Baird PA, Sadovnick AD, Yee IM. Maternal age and birth defects: a population
612 study. *Lancet.* 1991;337:527-530. doi: 10.1016/0140-6736(91)91306-f
- 613 4. Wang Z, Li L, Lei XY, Xue J, Mi HY. [Effect of advanced maternal age on birth
614 defects and postnatal complications of neonates]. *Zhongguo Dang Dai Er Ke Za*
615 *Zhi.* 2016;18:1084-1089.
- 616 5. Khairy P, Ionescu-Ittu R, Mackie AS, Abrahamowicz M, Pilote L, Marelli AJ.
617 Changing mortality in congenital heart disease. *J Am Coll Cardiol.*
618 2010;56:1149-1157. doi: 10.1016/j.jacc.2010.03.085
- 619 6. Thangaratnam S, Brown K, Zamora J, Khan KS, Ewer AK. Pulse oximetry
620 screening for critical congenital heart defects in asymptomatic newborn babies: a
621 systematic review and meta-analysis. *Lancet.* 2012;379:2459-2464. doi:
622 10.1016/S0140-6736(12)60107-X
- 623 7. Diller CL, Kelleman MS, Kupke KG, Quarry SC, Kochilas LK, Oster ME. A
624 Modified Algorithm for Critical Congenital Heart Disease Screening Using Pulse
625 Oximetry. *Pediatrics.* 2018;141. doi: 10.1542/peds.2017-4065

- 626 8. Mahle WT, Newburger JW, Matherne GP, Smith FC, Hoke TR, Koppel R,
627 Gidding SS, Beekman RH, 3rd, Grosse SD, American Heart Association
628 Congenital Heart Defects Committee of the Council on Cardiovascular Disease in
629 the Young CoCN, et al. Role of pulse oximetry in examining newborns for
630 congenital heart disease: a scientific statement from the American Heart
631 Association and American Academy of Pediatrics. *Circulation*. 2009;120:447-458.
632 doi: 10.1161/CIRCULATIONAHA.109.192576
- 633 9. Dalal A, Czosek RJ, Kovach J, von Alvensleben JC, Valdes S, Etheridge SP,
634 Ackerman MJ, Auld D, Huckaby J, McCracken C, et al. Clinical Presentation of
635 Pediatric Patients at Risk for Sudden Cardiac Arrest. *J Pediatr*. 2016;177:191-196.
636 doi: 10.1016/j.jpeds.2016.06.088
- 637 10. Kruska M, El-Battrawy I, Behnes M, Borggrefe M, Akin I. Biomarkers in
638 Cardiomyopathies and Prediction of Sudden Cardiac Death. *Curr Pharm
639 Biotechnol*. 2017;18:472-481. doi: 10.2174/1389201018666170623125842
- 640 11. Chatterjee D, Fatah M, Akdis D, Spears DA, Koopmann TT, Mittal K, Rafiq MA,
641 Cattanach BM, Zhao Q, Healey JS, et al. An autoantibody identifies
642 arrhythmogenic right ventricular cardiomyopathy and participates in its
643 pathogenesis. *Eur Heart J*. 2018;39:3932-3944. doi: 10.1093/eurheartj/ehy567
- 644 12. Coats CJ, Heywood WE, Mills K, Elliott PM. Current applications of biomarkers
645 in cardiomyopathies. *Expert Rev Cardiovasc Ther*. 2015;13:825-837. doi:
646 10.1586/14779072.2015.1053873
- 647 13. Fastner C, Behnes M, Sartorius B, Wenke A, Lang S, Yucel G, Sattler K, Rusnak
648 J, Saleh A, Barth C, et al. Interventional Left Atrial Appendage Closure Affects
649 the Metabolism of Acylcarnitines. *Int J Mol Sci*. 2018;19. doi:
650 10.3390/ijms19020500
- 651 14. Altit G, Bhombal S, Tacy TA, Chock VY. End-Organ Saturation Differences in
652 Early Neonatal Transition for Left- versus Right-Sided Congenital Heart Disease.
653 *Neonatology*. 2018;114:53-61. doi: 10.1159/000487472
- 654 15. Reddy S, Zhao M, Hu DQ, Fajardo G, Katznelson E, Punnett R, Spin JM, Chan FP,
655 Bernstein D. Physiologic and molecular characterization of a murine model of
656 right ventricular volume overload. *Am J Physiol Heart Circ Physiol*.
657 2013;304:H1314-1327. doi: 10.1152/ajpheart.00776.2012
- 658 16. Bove T, Vandekerckhove K, Bouchez S, Wouters P, Somers P, Van Nooten G.
659 Role of myocardial hypertrophy on acute and chronic right ventricular
660 performance in relation to chronic volume overload in a porcine model: relevance
661 for the surgical management of tetralogy of Fallot. *J Thorac Cardiovasc Surg*.
662 2014;147:1956-1965. doi: 10.1016/j.jtcvs.2013.10.026
- 663 17. Del Duca D, Wong G, Trieu P, Rodaros D, Kouremenos A, Tadevosyan A,
664 Vaniotis G, Villeneuve LR, Tchervenkov CI, Nattel S, et al. Association of
665 neonatal hypoxia with lasting changes in left ventricular gene expression: an
666 animal model. *J Thorac Cardiovasc Surg*. 2009;138:538-546, 546 e531. doi:
667 10.1016/j.jtcvs.2009.04.042

- 668 18. Liao P, Soong TW. CaV1.2 channelopathies: from arrhythmias to autism, bipolar
669 disorder, and immunodeficiency. *Pflugers Arch.* 2010;460:353-359. doi:
670 10.1007/s00424-009-0753-0
- 671 19. la Marca G, Carling RS, Moat SJ, Yahyaoui R, Ranieri E, Bonham JR, Schielen P.
672 Current State and Innovations in Newborn Screening: Continuing to Do Good and
673 Avoid Harm. *Int J Neonatal Screen.* 2023;9. doi: 10.3390/ijns9010015
- 674 20. Sinclair TJ, Ye C, Chen Y, Zhang D, Li T, Ling XB, Cohen HJ, Shaw GM,
675 Stevenson DK, Chace D, et al. Progressive Metabolic Dysfunction and Nutritional
676 Variability Precedes Necrotizing Enterocolitis. *Nutrients.* 2020;12. doi:
677 10.3390/nu12051275
- 678 21. Zhu L, Huang Q, Li X, Jin B, Ding Y, Chou CJ, Su KJ, Zhang Y, Chen X, Hwa
679 KY, et al. Serological Phenotyping Analysis Uncovers a Unique Metabolomic
680 Pattern Associated With Early Onset of Type 2 Diabetes Mellitus. *Front Mol*
681 *Biosci.* 2022;9:841209. doi: 10.3389/fmolb.2022.841209
- 682 22. Kanehisa M, Furumichi M, Sato Y, Ishiguro-Watanabe M, Tanabe M. KEGG:
683 integrating viruses and cellular organisms. *Nucleic Acids Res.*
684 2021;49:D545-D551. doi: 10.1093/nar/gkaa970
- 685 23. Fahy E, Subramaniam S, Murphy RC, Nishijima M, Raetz CR, Shimizu T, Spener
686 F, van Meer G, Wakelam MJ, Dennis EA. Update of the LIPID MAPS
687 comprehensive classification system for lipids. *J Lipid Res.* 2009;50 Suppl:S9-14.
688 doi: 10.1194/jlr.R800095-JLR200
- 689 24. Bradshaw CJA, Herrando-Perez S. Logistic-growth models measuring density
690 feedback are sensitive to population declines, but not fluctuating carrying capacity.
691 *Ecol Evol.* 2023;13:e10010. doi: 10.1002/ece3.10010
- 692 25. Peng Y, Zhao S, Zeng Z, Hu X, Yin Z. LGBMDF: A cascade forest framework
693 with LightGBM for predicting drug-target interactions. *Front Microbiol.*
694 2022;13:1092467. doi: 10.3389/fmicb.2022.1092467
- 695 26. Ke G, Meng Q, Finley T, Wang T, Chen W, Ma W, Ye Q, Liu T-Y. LightGBM: a
696 highly efficient gradient boosting decision tree. In: *Proceedings of the 31st*
697 *International Conference on Neural Information Processing Systems.* Long Beach,
698 California, USA: Curran Associates Inc.; 2017:3149–3157.
- 699 27. Hakuno D, Hamba Y, Toya T, Adachi T. Plasma amino acid profiling identifies
700 specific amino acid associations with cardiovascular function in patients with
701 systolic heart failure. *PLoS One.* 2015;10:e0117325. doi:
702 10.1371/journal.pone.0117325
- 703 28. Fukushima A, Zhang L, Huqi A, Lam VH, Rawat S, Altamimi T, Wagg CS,
704 Dhaliwal KK, Hornberger LK, Kantor PF, et al. Acetylation contributes to
705 hypertrophy-caused maturational delay of cardiac energy metabolism. *JCI Insight.*
706 2018;3. doi: 10.1172/jci.insight.99239
- 707 29. Wang B, Wu L, Chen J, Dong L, Chen C, Wen Z, Hu J, Fleming I, Wang DW.
708 Metabolism pathways of arachidonic acids: mechanisms and potential therapeutic
709 targets. *Signal Transduct Target Ther.* 2021;6:94. doi:
710 10.1038/s41392-020-00443-w

- 711 30. Yang LG, Song ZX, Yin H, Wang YY, Shu GF, Lu HX, Wang SK, Sun GJ. Low
712 n-6/n-3 PUFA Ratio Improves Lipid Metabolism, Inflammation, Oxidative Stress
713 and Endothelial Function in Rats Using Plant Oils as n-3 Fatty Acid Source.
714 *Lipids*. 2016;51:49-59. doi: 10.1007/s11745-015-4091-z
- 715 31. Kanoh M, Inai K, Shinohara T, Tomimatsu H, Nakanishi T. Clinical implications
716 of eicosapentaenoic acid/arachidonic acid ratio (EPA/AA) in adult patients with
717 congenital heart disease. *Heart Vessels*. 2017;32:1513-1522. doi:
718 10.1007/s00380-017-1015-2
- 719 32. Tian W, Jiang X, Tamosiuniene R, Sung YK, Qian J, Dhillon G, Gera L, Farkas L,
720 Rabinovitch M, Zamanian RT, et al. Blocking macrophage leukotriene b4 prevents
721 endothelial injury and reverses pulmonary hypertension. *Sci Transl Med*.
722 2013;5:200ra117. doi: 10.1126/scitranslmed.3006674
- 723 33. Vrigkou E, Tsantes AE, Kopterides P, Orfanos SE, Armaganidis A, Maratou E,
724 Rapti E, Pappas A, Tsantes AG, Tsangaris I. Coagulation Profiles of Pulmonary
725 Arterial Hypertension Patients, Assessed by Non-Conventional Hemostatic Tests
726 and Markers of Platelet Activation and Endothelial Dysfunction. *Diagnostics*
727 (*Basel*). 2020;10. doi: 10.3390/diagnostics10100758
- 728 34. Gu H, Fang YJ, Liu DD, Chen P, Mei YA. cAMP/PKA Pathways and S56
729 Phosphorylation Are Involved in AA/PGE2-Induced Increases in rNaV1.4
730 Current. *PLoS One*. 2015;10:e0140715. doi: 10.1371/journal.pone.0140715
- 731 35. Lai J, Chen C. The Role of Epoxyeicosatrienoic Acids in Cardiac Remodeling.
732 *Front Physiol*. 2021;12:642470. doi: 10.3389/fphys.2021.642470
- 733 36. Evangelista EA, Aliwarga T, Sotoodehnia N, Jensen PN, McKnight B, Lemaitre
734 RN, Totah RA, Gharib SA. CYP2J2 Modulates Diverse Transcriptional Programs
735 in Adult Human Cardiomyocytes. *Sci Rep*. 2020;10:5329. doi:
736 10.1038/s41598-020-62174-w
- 737 37. Li N, Liu JY, Qiu H, Harris TR, Sirish P, Hammock BD, Chiamvimonvat N. Use
738 of metabolomic profiling in the study of arachidonic acid metabolism in
739 cardiovascular disease. *Congest Heart Fail*. 2011;17:42-46. doi:
740 10.1111/j.1751-7133.2010.00209.x
- 741 38. Levick SP, Loch DC, Taylor SM, Janicki JS. Arachidonic acid metabolism as a
742 potential mediator of cardiac fibrosis associated with inflammation. *J Immunol*.
743 2007;178:641-646. doi: 10.4049/jimmunol.178.2.641
- 744 39. Aslibekyan S, Jensen MK, Campos H, Linkletter CD, Loucks EB, Ordovas JM,
745 Deka R, Rimm EB, Baylin A. Fatty Acid desaturase gene variants, cardiovascular
746 risk factors, and myocardial infarction in the costa rica study. *Front Genet*.
747 2012;3:72. doi: 10.3389/fgene.2012.00072
- 748 40. Pahnke A, Conant G, Huyer LD, Zhao Y, Feric N, Radisic M. The role of Wnt
749 regulation in heart development, cardiac repair and disease: A tissue engineering
750 perspective. *Biochem Biophys Res Commun*. 2016;473:698-703. doi:
751 10.1016/j.bbrc.2015.11.060
- 752 41. Wang J, Liang Y, Jian L, Zhang J, Liang S, Xiao S, Liu B, Wang H. Linoelaidic
753 acid enhances adipogenic differentiation in adipose tissue-derived stromal cells
754 through suppression of Wnt/beta-catenin signaling pathway in vitro.

- 755 *Prostaglandins Leukot Essent Fatty Acids*. 2016;110:1-7. doi:
756 10.1016/j.plefa.2016.04.004
- 757 42. Mohamed IA, El-Badri N, Zaher A. Wnt Signaling: The double-edged sword
758 diminishing the potential of stem cell therapy in congenital heart disease. *Life Sci*.
759 2019;239:116937. doi: 10.1016/j.lfs.2019.116937
- 760 43. Dekker Nitert M, Vaswani K, Hum M, Chan HW, Wood-Bradley R, Henry S,
761 Armitage JA, Mitchell MD, Rice GE. Maternal high-fat diet alters expression of
762 pathways of growth, blood supply and arachidonic acid in rat placenta. *J Nutr Sci*.
763 2013;2:e41. doi: 10.1017/jns.2013.36
- 764 44. Lee SH, Kim MH, Han HJ. Arachidonic acid potentiates hypoxia-induced VEGF
765 expression in mouse embryonic stem cells: involvement of Notch, Wnt, and
766 HIF-1alpha. *Am J Physiol Cell Physiol*. 2009;297:C207-216. doi:
767 10.1152/ajpcell.00579.2008
- 768 45. Lambrechts D, Carmeliet P. Genetics in zebrafish, mice, and humans to dissect
769 congenital heart disease: insights in the role of VEGF. *Curr Top Dev Biol*.
770 2004;62:189-224. doi: 10.1016/S0070-2153(04)62007-2
- 771 46. Smedts HP, Rakhshandehroo M, Verkleij-Hagoort AC, de Vries JH, Ottenkamp J,
772 Steegers EA, Steegers-Theunissen RP. Maternal intake of fat, riboflavin and
773 nicotinamide and the risk of having offspring with congenital heart defects. *Eur J*
774 *Nutr*. 2008;47:357-365. doi: 10.1007/s00394-008-0735-6
- 775 47. Smedts HP, van Uitert EM, Valkenburg O, Laven JS, Eijkemans MJ, Lindemans J,
776 Steegers EA, Steegers-Theunissen RP. A derangement of the maternal lipid profile
777 is associated with an elevated risk of congenital heart disease in the offspring. *Nutr*
778 *Metab Cardiovasc Dis*. 2012;22:477-485. doi: 10.1016/j.numecd.2010.07.016
- 779 48. Burgoyne JR, Mongue-Din H, Eaton P, Shah AM. Redox signaling in cardiac
780 physiology and pathology. *Circ Res*. 2012;111:1091-1106. doi:
781 10.1161/CIRCRESAHA.111.255216
- 782 49. Manso PH, Carmona F, Dal-Pizzol F, Petronilho F, Cardoso F, Castro M, Carlotti
783 AP. Oxidative stress markers are not associated with outcomes after pediatric heart
784 surgery. *Paediatr Anaesth*. 2013;23:188-194. doi: 10.1111/pan.12040
- 785 50. Calza G, Lerzo F, Perfumo F, Borini I, Panizzon G, Moretti R, Grasso P, Virgone
786 A, Zannini L. Clinical evaluation of oxidative stress and myocardial reperfusion
787 injury in pediatric cardiac surgery. *J Cardiovasc Surg (Torino)*. 2002;43:441-447.
- 788 51. Nydegger A, Bines JE. Energy metabolism in infants with congenital heart
789 disease. *Nutrition*. 2006;22:697-704. doi: 10.1016/j.nut.2006.03.010
- 790 52. Sun X, Sharma S, Fratz S, Kumar S, Rafikov R, Aggarwal S, Rafikova O, Lu Q,
791 Burns T, Dasarathy S, et al. Disruption of endothelial cell mitochondrial
792 bioenergetics in lambs with increased pulmonary blood flow. *Antioxid Redox*
793 *Signal*. 2013;18:1739-1752. doi: 10.1089/ars.2012.4806
- 794 53. Black SM, Field-Ridley A, Sharma S, Kumar S, Keller RL, Kameny R, Maltepe E,
795 Datar SA, Fineman JR. Altered Carnitine Homeostasis in Children With Increased
796 Pulmonary Blood Flow Due to Ventricular Septal Defects. *Pediatr Crit Care Med*.
797 2017;18:931-934. doi: 10.1097/PCC.0000000000001275

798 54. Bahado-Singh RO, Ertl R, Mandal R, Bjorndahl TC, Syngelaki A, Han B, Dong E,
799 Liu PB, Alpay-Savasan Z, Wishart DS, et al. Metabolomic prediction of fetal
800 congenital heart defect in the first trimester. *Am J Obstet Gynecol.* 2014;211:240
801 e241-240 e214. doi: 10.1016/j.ajog.2014.03.056

802

Figure 1.

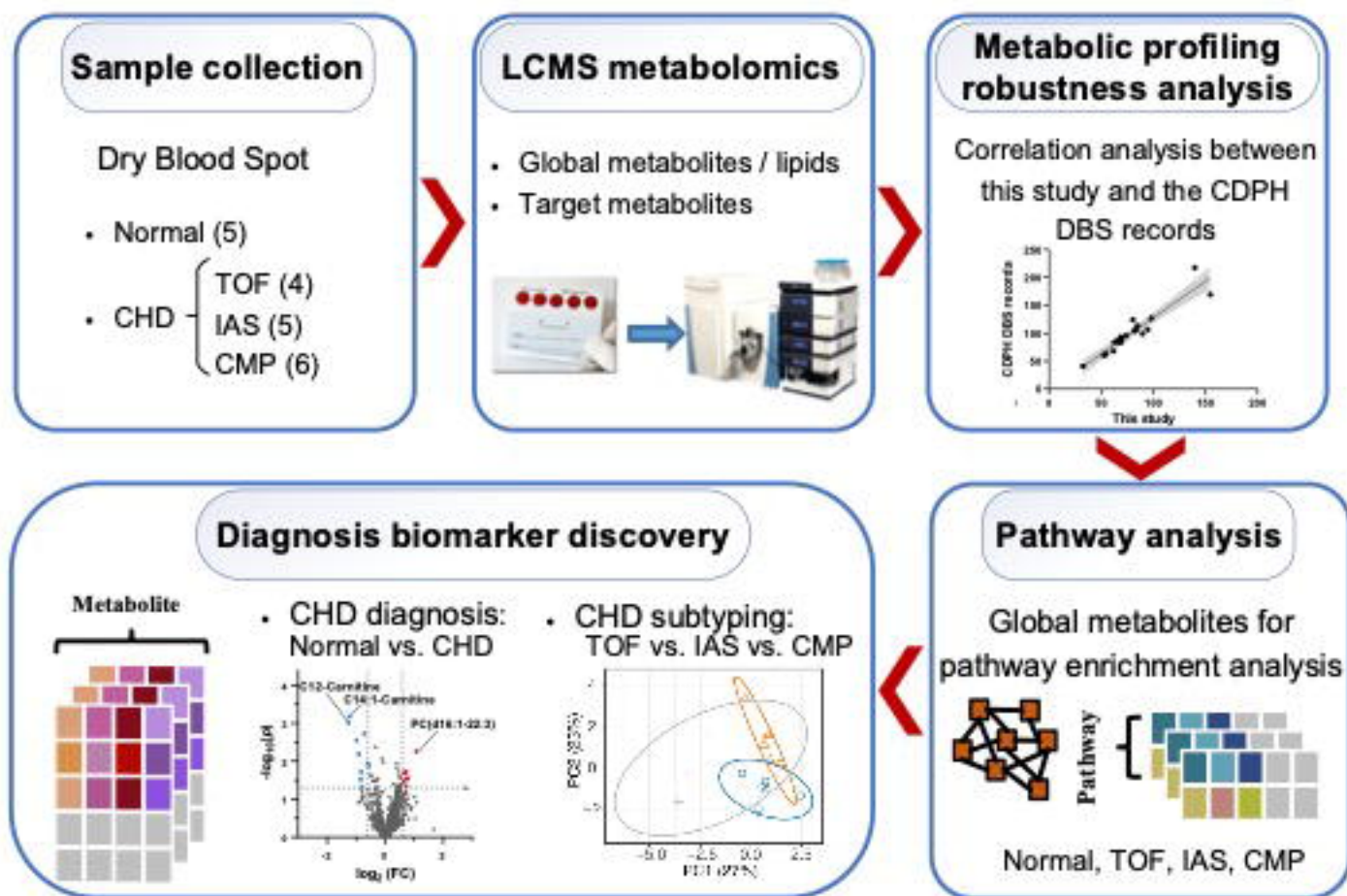


Figure 2.

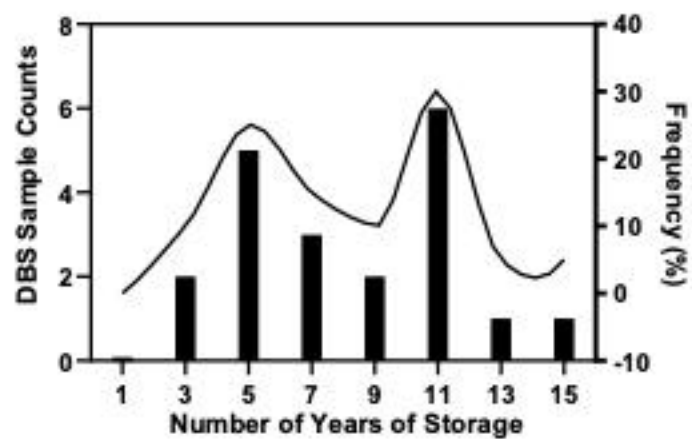


Figure 3.

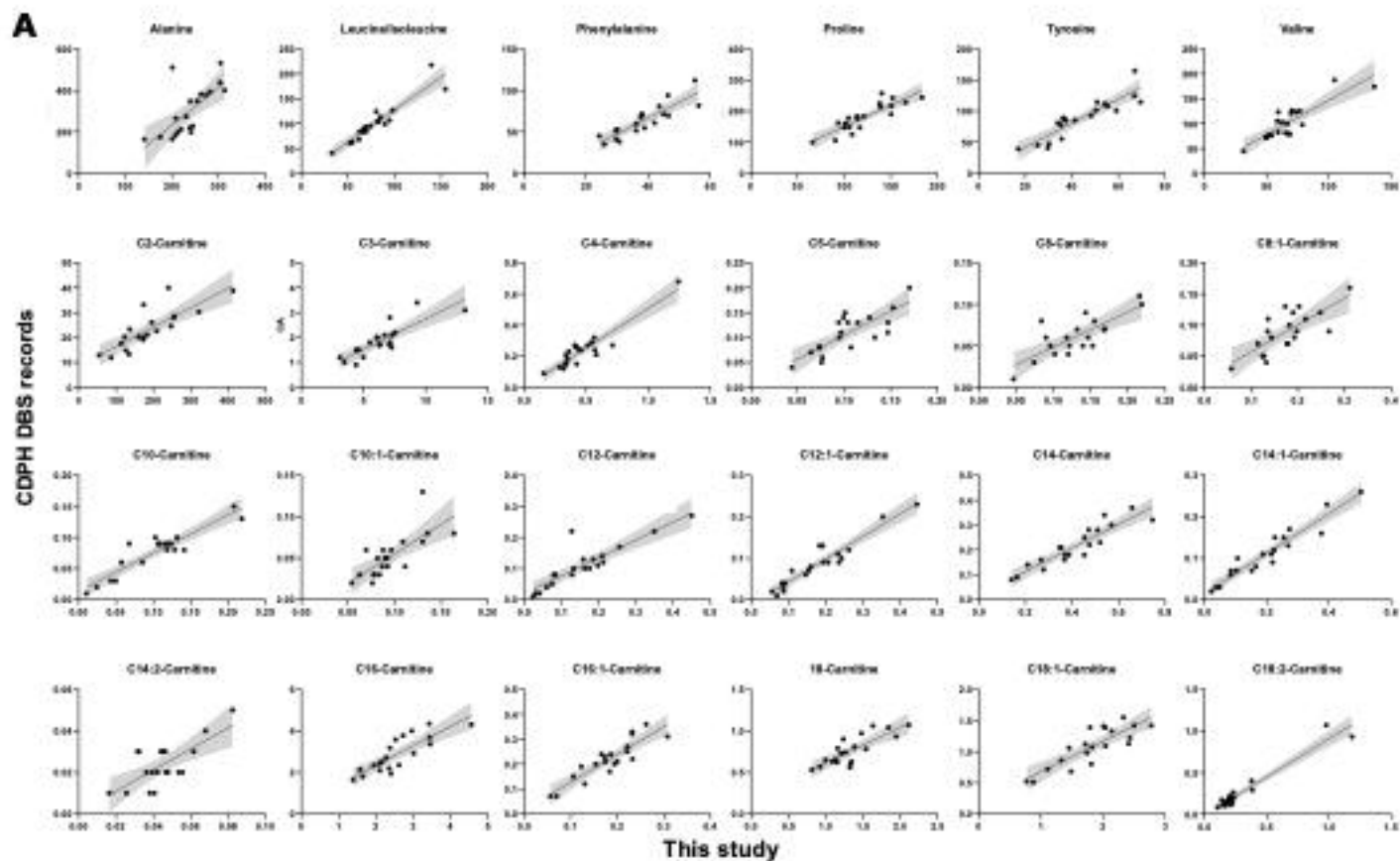


Figure 3.

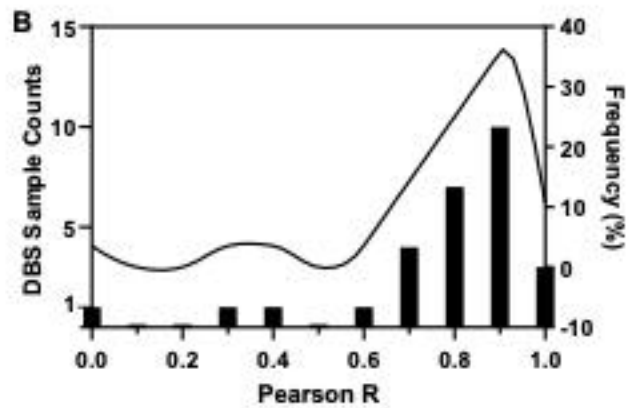


Figure 4.

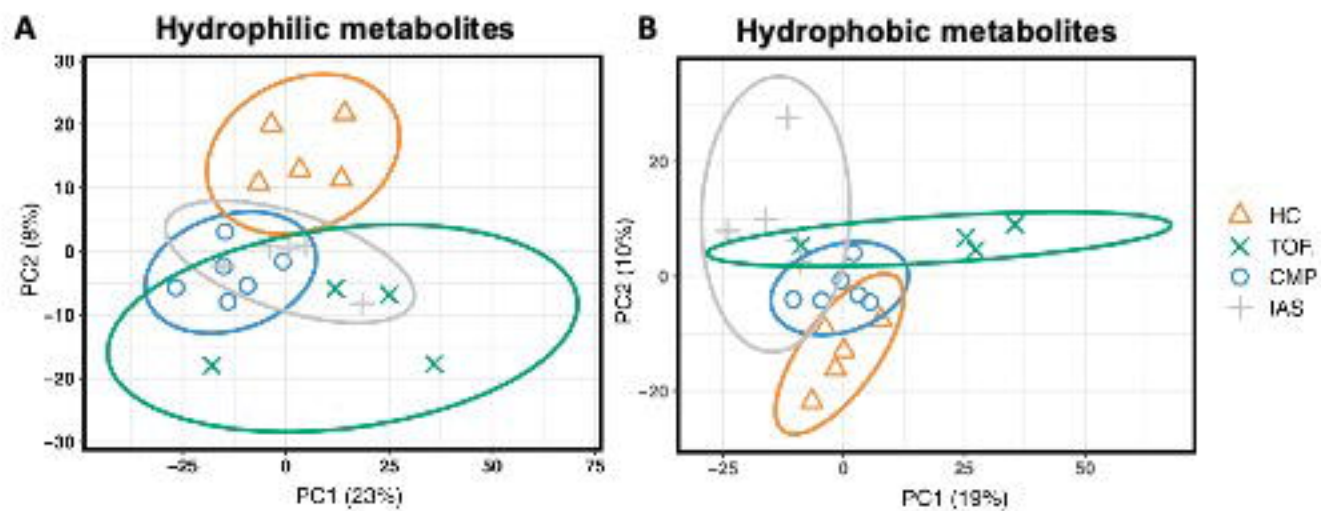


Figure 5.

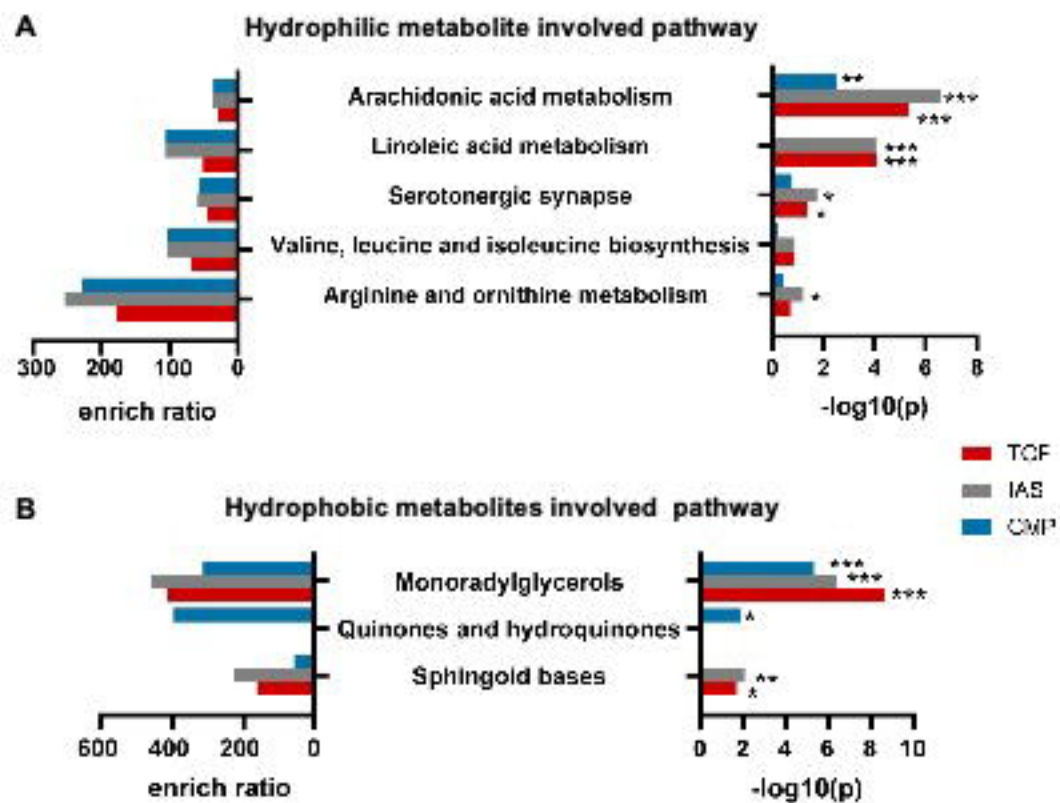


Figure 6.